PROCEEDINGS of the
23rd International Congress on Acoustics
9 to 13 September 2019 in Aachen, Germany

Determination of frequency dependent ultrasound absorption by means of radiation force based power measurements

Tina A. FUHRMANN[(1)], Konrad MEHLE[(1)], David WALTSCHEW[(1)], Klaus-V. JENDERKA[(1)]

[(1)]University of Applied Sciences Merseburg, Department of Engineering and Natural Sciences, Germany,
tina.fuhrmann@hs-merseburg.de

Abstract

Frequency dependent acoustic absorption of propagating ultrasound waves is a key quantity in acoustic material characterization. The standard approaches to determine the amplitude absorption coefficient either analyze the amplitude decay of subsequent rear surface reflections of a sample with known thickness (materials with low acoustic absorption) or the insertion loss of samples with different thicknesses (materials with higher acoustic absorption). Our new approach uses the total temporal averaged ultrasonic power determined by means of a Radiation Force Balance, by comparing the power values of excited bursts (number of cycles > 100) with and without the sample. The required information about the thickness and speed of sound of the sample, as well as consequently the amplitude reflection and transmission coefficients, were determined in advance within the same measurement setup. The effects of half-wave layers on the reflection and transmission coefficients are incorporated in the analyzing routines. Additionally, the frequencies of the resulting peaks of transmitted power can be used for refinement of the samples thickness or speed-of-sound measurements. Determining ultrasound absorption by means of Radiation Force based power measurements takes advantage of the low uncertainty of the method, but requires an extended time frame for the measurements.

Keywords: Absorption, Attenuation, Speed of Sound, Radiation Force Balance, Acoustic Material Properties

1 INTRODUCTION

The knowledge of acoustic material properties is important to develop new and improve existing ultrasound technologies, for instance clamp-on sensors in the medical field. They are used in diagnostics e.g. for blood flow measurements or bubble detection. The sensors are directly connected to the blood-carrying tubes and therefore the measurement accuracy, as well as the feasibility of quantitative measurements in general, strongly depends on the knowledge of the tube properties and the correct configuration of the sensors on the basis of these properties. Hence the tubes properties must be measured accurately in advance.

Material quantities of interest usually are the speed of sound, impedance, and attenuation or absorption, as well as the thickness and density. A compromise has to be made between accuracy, and time and effort spent on the measurement. To access the attenuation, two methods are common [1]: The first is the *single sample through transmission method* where the amplitude decay of subsequent rear surface reflections is analyzed. The sample's thickness must be known and its absorption must be smaller to allow multiple reflections. The second is the *double sample through transmission method* which uses the insertion loss of at least two samples with different thicknesses and is used for materials with higher acoustic absorption. To obtain small uncertainties, big efforts have to be made concerning the measurement setup (placement and alignment of equipment), the experimental execution and to meet the narrow conditions under which all the assumptions are valid. Those conditions are the use of very short pulses, a narrow sound field geometry, and the exact determination of the acoustic impedance to calculate the transmission and

reflection coefficients. It also requires the exact determination of the sample's speed of sound and density.

In our approach all the above mentioned quantities - absorption, thickness, density, speed of sound, and impedance of the sample - are measured very accurately and combined in only one measurement setup. For the absorption measurement a radiation force balance (RFB) is used. Very short pulses are replaced by very long ones, which results in a higher ultrasonic power available for measurement and therefore more accurate readings. It also implies the usage of a total transmission and reflection coefficient, respectively, that takes all transmitted and reflected echoes into account. In ultrasound metrology the lowest uncertainties (about 3 %) can be achieved for measurement of the total temporal averaged ultrasonic power.

Our samples are made of PMMA (polymethacrylate) because it is often used as buffer rod, for ultrasound and radiation therapy phantoms, as well as for comparison measurements. Its ultrasound properties can be found in literature [2, 3, 4].

2 THEORY

2.1 Density Measurement

For the density measurement the buoyancy of the sample in water is used and therefore requires only a balance. With the measured mass of the sample in air m_S and in water $m_{S,w}$ as well as the known density of water at a given temperature ϱ_w from [5] the density ϱ_S of the sample can be calculated:

$$\varrho_s = \frac{m_S \cdot \varrho_w}{m_S - m_{S,w}} \tag{1}$$

This results from the equilibrium of buoyancy force from the sample $F_{S,b} = \varrho_w V_S g$ and the weight force $F_{w,g} = m_W g$, with g being the constant of gravitational acceleration. Then immediately

$$V_S = \frac{m_S}{\varrho_S} = \frac{m_w}{\varrho_w} = \frac{m_S - m_{S,w}}{\varrho_w} \tag{2}$$

follows, which finally results in equation 1.

2.2 Speed of sound and Thickness Measurement

To measure the speed of sound and thickness of the sample a pulse-echo method is used [6].

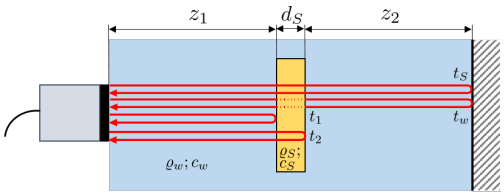

Figure 1. Measurement of thickness and speed of sound of the sample. Here d_S is the thickness of the sample, z_1 and z_2 the ultrasound path lengths in front and behind the sample, t_1 and t_2 the runtimes of ultrasound to the front and back wall of the sample, and t_S and t_w the runtimes to the ultrasound reflector with and without the sample in the ultrasound path, respectively.

The experimental setup and runtimes of interest are shown in figure 1. They are defined by

$$t_1 = 2 \cdot \frac{z_1}{c_w} \tag{3}$$

$$t_2 = 2 \cdot \frac{z_1}{c_w} + 2 \cdot \frac{d_S}{c_S} \tag{4}$$

$$t_w = 2 \cdot \frac{z_1}{c_w} + 2 \cdot \frac{d_S}{c_w} + 2 \cdot \frac{z_2}{c_w} \tag{5}$$

$$t_S = 2 \cdot \frac{z_1}{c_w} + 2 \cdot \frac{d_S}{c_S} + 2 \cdot \frac{z_2}{c_w} \tag{6}$$

and for the calculations the temperature dependent speed of sound from water published in [7] is used. The runtimes are given through measurement and the unknown variables are d_S and c_S as well as z_1 and z_2:

$$c_S = c_w \cdot \left(\frac{t_w - t_S}{t_2 - t_1} + 1 \right) \tag{7}$$

$$d_S = c_S \cdot \frac{t_2 - t_1}{2} \tag{8}$$

2.3 Absorption Measurement

The absorption measurement is done in transmitting mode. A large absorbing target, which is connected to a balance, absorbs almost the whole acoustic power that reaches the target. The front face of the ultrasound transducer, the sample's, and the absorber's surfaces are aligned parallel.

With our measurement setup (section 3) we measure, strictly speaking, the attenuation within the probe. However, the following conditions allow the assumption that attenuation is only due to absorption and therefore the terms can be used equivalently in this paper:

- The front and back walls of our samples are parallel to each other and perpendicular to the center line of ultrasound propagation. Therefore the incident and emerging ultrasound angles are 90° and no energy is reflected or scattered out of the absorbing target due to geometrical conditions of the sample.
- The material examined in this investigation (PMMA) is in a good approximation homogeneous and free from scatterers. Therefore no ultrasound energy is scattered out of the target area due to scattering within the sample.

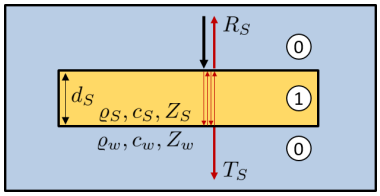

Figure 2. The sample is shown in yellow with its thickness d_S. For the theoretical derivation of the reflection and transmission coefficients R_S and T_S with extended (infinite) ultrasound pulses the indices 0 and 1 are used for water and the sample, respectively.

To derive the (complex) amplitude transmission coefficient we start by taking into account the first transmission through the sample [8]. The ultrasound wave enters the sample (transmission coefficient T_{01}), passes through it and emerges on the opposite side (T_{10}). Considering the advance of the phase e^{ikd_S} and the absorption $e^{-\alpha d_S}$, the total transmission coefficient is given by

$$T_S = T_{01}T_{10} \cdot e^{ik_S d_S} e^{-\alpha d_S} \tag{9}$$

If k has an imaginary part, then the factor $e^{ik_S d_S}$ also adds attenuation to the transmission coefficient. Next, also the reflection at the lower boundary R_{10} (figure 2), the inner passage through the sample, the reflection at the upper boundary (R_{10}) and another passage through the sample are included:

$$T_S = T_{01}T_{10} \cdot e^{ik_S d_S} e^{-\alpha d_S} + T_{01}R_{10}R_{10}T_{10} \cdot e^{3ik_S d_S} e^{-3\alpha d_S} \tag{10}$$

Note that possible phase jumps are represented by the sign of the reflection coefficient. When considering an infinite amount of reflections within the probes, we finally we come to the formula

$$\begin{aligned} T_S &= T_{01}T_{10} \cdot e^{ik_S d_S} e^{-\alpha d_S} \\ &\quad + T_{01}T_{10} \cdot e^{ik_S d_S} e^{-\alpha d_S} \cdot R_{10}R_{10} \cdot e^{2ik_S d_S} e^{-2\alpha d_S} \\ &\quad + T_{01}T_{10} \cdot e^{ik_S d_S} e^{-\alpha d_S} \cdot \left(R_{10}R_{10} \cdot e^{2ik_S d_S} e^{-2\alpha d_S}\right)^2 \\ &\quad + \ldots \\ &= T_{01}T_{10} \cdot e^{ik_S d_S} e^{-\alpha d_S} \cdot \lim_{m\to\infty} \sum_{l=0}^{m} \left(R_{10}^2 \cdot e^{2ik_S d_S} e^{-2\alpha d_S}\right)^l, \qquad l \in \mathbb{N}_0 \end{aligned} \tag{11}$$

This is an infinite series in the form $S_l = \lim\limits_{m\to\infty} \sum\limits_{l=0}^{m} x^l$ which is given by $S_l = \lim\limits_{l\to\infty} \frac{1-x^l}{1-x} = \frac{1}{1-x}$ for all $|x| < 1$. The term $\left(R_{10}^2 \cdot e^{2ik_S d_S} e^{-2\alpha d_S}\right)$ is always smaller than 1 because each factor is smaller than 1 and $|e^{2ik_S d_S}| \leq 1$, respectively. Therefore the transmission and, analogously, the reflection coefficients are

given by

$$T_S = \frac{T_{01}T_{10} \cdot e^{ik_S d_S} e^{-\alpha d_S}}{1 - R_{10}^2 \cdot e^{2ik_S d_S} e^{-2\alpha d_S}} \tag{12}$$

$$R_S = R_{01} + \frac{T_{01}R_{10}T_{10} \cdot e^{2ik_S d_S} e^{-2\alpha d_S}}{1 - R_{10}^2 \cdot e^{2ik_S d_S} e^{-2\alpha d_S}} \tag{13}$$

With the known densities and speeds of sound from water (ϱ_w[5],c_w[7]) and the sample (ϱ_S,c_S; see sections 2.1 and 2.2) the transmission and reflection coefficients for the water-sample border (T_{01}, R_{01}) can be calculated from the acoustic impedances ($Z = \varrho\, c$):

$$T_{01} = \frac{2Z_S}{Z_S + Z_w} \tag{14}$$

$$R_{01} = \frac{Z_S - Z_w}{Z_S + Z_w} \tag{15}$$

With the radiation force balance, the ultrasonic power P received at an absorbing target is determined through measurement of the mass "jumps" $P = c_W \cdot g \cdot \Delta m$ when turning the ultrasound transducer on. Therefore the absorption can be obtained by numerically fitting the equation

$$\sqrt{\frac{P_S}{P_e}} = \sqrt{\frac{c_w(\vartheta) \cdot \Delta m_S}{c_w(\vartheta) \cdot \Delta m_e}} = \frac{T_{01}T_{10} \cdot e^{ik_S d_S} e^{-\alpha d_S}}{1 - R_{10}^2 \cdot e^{2ik_S d_S} e^{-2\alpha d_S}} \tag{16}$$

with P_S and P_e being the measured ultrasound powers at the radiation force balance with and without the sample in the ultrasound path, $c_W(\vartheta)$ the temperature dependent speed of sound of water, and Δm_S and Δm_e the mass differences when turning on the ultrasound transducer with and without the sample in the ultrasound path. For α we use the general formula

$$\alpha = a \cdot f^b \tag{17}$$

with a and b being constants and f being the frequency.

2.4 Half-wave layers

In the previous section the transmission and reflection coefficients for infinite ultrasound waves were derived. Since the wave has an infinite length it is important to add the phases correctly. This is done by the term $e^{2ik_S d_S}$ and immediately leads to effects that provide further information.
First it predicts half-wave layers at sample thicknesses $d_S = \frac{m\lambda_S}{2} = \frac{m\pi}{k_S}$ (with $m = 1, 2, ...$). From the equations 12 and 13 it can be easily seen that (by neglecting the absorption) the transmission coefficient $T_S = 1$ and $R_S = 0$ (using the relations $e^{ik_S d_S} = \cos(k_S d_S) + i\sin(k_S d_S)$, $T_{01} = 1 + R_{01}$ and $R_{01} = R_{10}$). Taking the absorption into account it still holds that the transmission coefficient has a maximum at those frequencies where the sample thickness corresponds to half a wavelength ($f = \frac{mc_S}{2d_S}$) and the reflection coefficient a minimum.
It secondly means, that an oscillation of the ultrasonic power is present in the spectrum that is only dependent on the speed of sound of the sample and its thickness. It can therefore be used to refine one of those measurements, whichever is less accurate. A detailed analysis and proof of concept are beyond the scope of this paper and will be included in detail in future work.

3 EXPERIMENTAL SETUP, CALCULATION, AND MATERIAL

In figure 3 the experimental setup is shown: measurement of absorption/attenuation - reflector open, measurement of speed of sound and sample thickness - reflector closed.

Absorption measurement

To determine the ultrasonic power a radiation force balance (RFB) method as described in [9] is used. The setup is equal to the RFB setup in [10] used by PTB and has an uncertainty of about 3% at 5 MHz. The ultrasound transducer (Olympus, diameter 5 MHz, 12.7 mm (0.5 inch), bandwidth 3.14 MHz) is oriented upward and run by a generator (Tektronix AFG3101) and amplifier (121CR rf power labs, 50 dB) in transmit-mode sending 2 μs bursts at a single frequency. The target (HAM A, Precision Acoustics) is placed 10 cm above the transducer covering the whole cross section of the ultrasonic field and absorbs 99% of the received ultrasound energy. The mass difference is measured with a balance (AX105 Delta Range from Mettler-Toledo, $\Delta m = 0.1$ mg). The experiments are run and analyzed with MATLAB 2019b. Temperature was controlled with the thermometer GMH 3710 from Greisinger electronic.

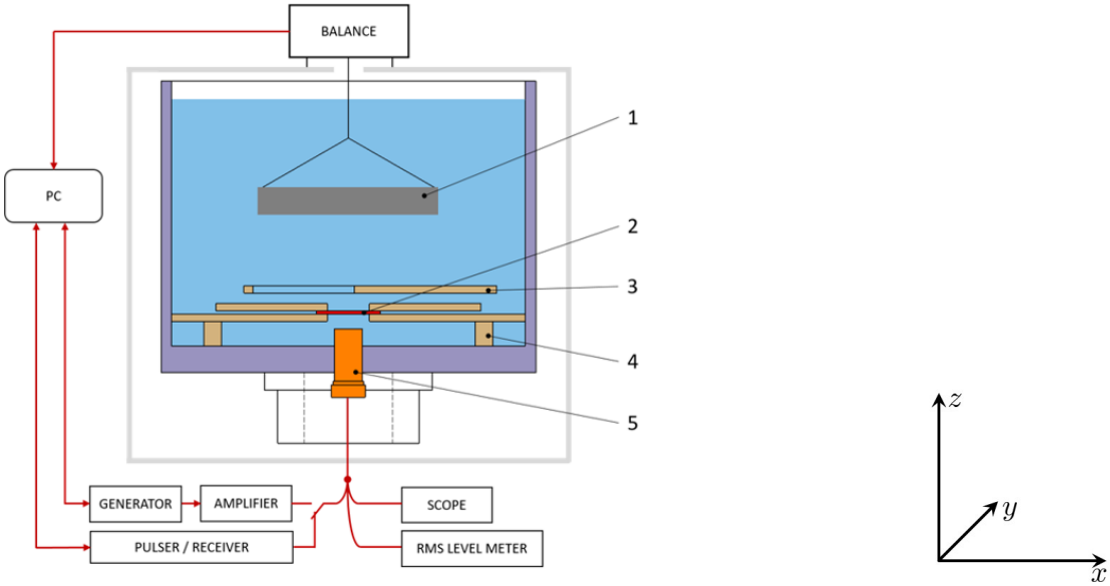

Figure 3. Measurement of attenuation. 1..absorbing target, 2..sample, 3..laterally displaceable reflector, 4..sample holder, 5..transducer

Absorption calculation
A numerical fit of equation 16, using equations 12 to 17, was used to calculate the coefficients a and b of the absorption $\alpha = a \cdot f^b$. Using MATLAB 2019b, the sum of the squared residuals was minimized. The increments of a and b where 0.001 and 0.01, respectively. Since a frequency exponent very close to 1 was found, the fit model for the hydrophone measurements was changed to $\alpha = c + a \cdot f$.

Speed of sound and thickness measurement
A pulser-receiver (Panametrics Model 5800) runs the US-transducer and emits bursts of three cycles. The received signal is send to an oscilloscope (Keysight InfiniiVision DSO-X 3034T) and read out by MATLAB. The reflector can be moved along the x-direction into the sound field.

Hydrophone measurement
The US transducer is placed downwards in a degassed waterbath (temperature and oxygen measurement with Hach HQ 40d). The hydrophone (ONDA HGL-0400 S/N 1380, effective diameter 0.4 mm) is placed in the distance of 15 cm from the transducer. The transducer is run with a function generator (Agilent 33 220 A) and the hydrophone signal is acquired with an oscilloscope (PicoScope PS5244A) and processed by the ONDA software Sonic Software for AIMS III, Ver. 5.2.4.0.

Samples
For this paper different PMMA discs of thicknesses 2 mm, 3 mm, 5 mm, 7.5 mm, and 10 mm were used. PMMA is a suitable plastic for comparative measurements and for verifying the new measurement configuration.

4 RESULTS

4.1 PMMA data

At least three independent measurements were made at room temperature for each mentioned property. The results for density, sample thickness and speed of sound measurements of the PMMA discs are shown in table 1. In addition, the calculated impedances, uncertainties, and mean values are presented.

4.2 Power Measurement and Absorption

The ultrasonic power was measured at room temperature once per sample with the radiation force balance method as a proof of concept. The results are shown in figure 4. More experiments, as well as a detailed uncertainty consideration, will be subject to a following paper. For comparison reasons, the ultrasound peak-to-peak pressure was measured three times per sample with a hydrophone and is also

Table 1. The thicknesses were measured with a caliper (†) and the ultrasound method (‡). Density, thickness^2, and speed of sound of the PMMA discs were calculated with equations 1, 8, and 7. In the last row the average values $\overline{x}$ plus-minus the standard deviations σ are shown.

sample	thickness† (mm)	thickness‡ (mm)	mass (kg)	density (kg/m^3)	speed of sound (m/s)	impedance (Mrayl)
PMMA 2	2.00	1.996	6.674	1185	2732	3.240
PMMA 3	3.00	2.987	9.970	1186	2740	3.249
PMMA 5	5.02	5.009	16.78	1186	2755	3.267
PMMA 7.5	7.51	7.513	25.11	1186	2754	3.266
PMMA 10	10.01	10.00	33.44	1186	2739	3.248
$\overline{x}$				1186	2744	3.254
uncertainty	$\leq 0.1\%$	$\leq 0.2\,\%$	0.001 g	1 kg/m^3 = 0.8‰	$\leq 0.4\,\%$	$\leq 0.4\,\%$

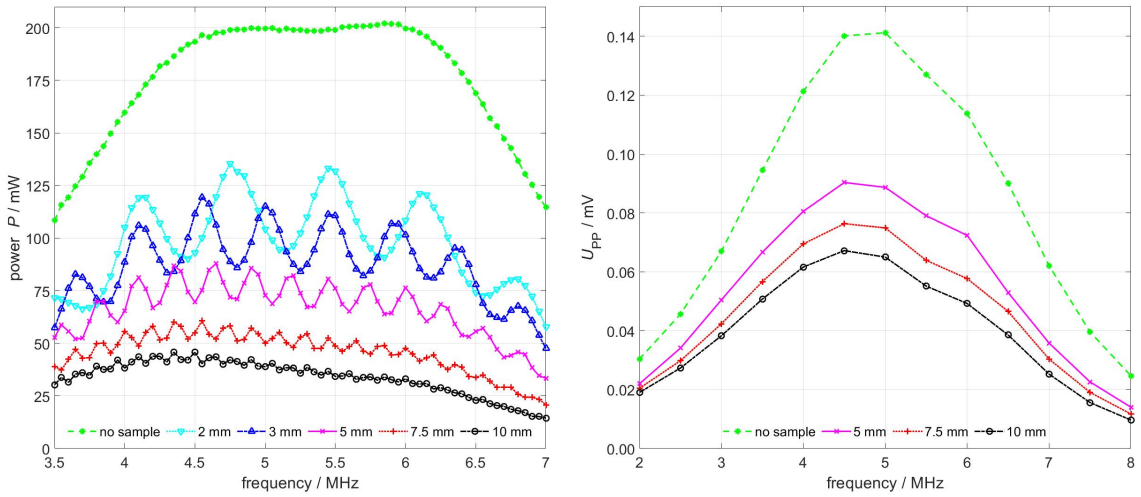

(a) Radiation Force Balance

(b) Hydrophone

Figure 4. Ultrasonic power measured with the radiation force balance (a) and hydrophone (b) of PMMA discs of different thicknesses. Reference measurements in water without PMMA samples. Absorption values are listed in table 2.

shown in figure 4. The method used is not suitable for very small absorptions and therefore the inaccurate measurements at 2 mm and 3 mm are evaluated.

Table 2. Absorption of PMMA samples at room temperature measured with the radiation force balance ($\alpha = a \cdot f^b$) as well as a hydrophone ($\alpha = c + a \cdot f$). Values at 5 MHz are calculated. See also figure 4.

sample	Radiation Force Balance a (dB/(cm MHz^b))	b	$\alpha_{(5\,\mathrm{MHz})}$ (dB/cm)	Hydrophone a (dB/(cm MHz))	c (dB/cm)	$\alpha_{(5\,\mathrm{MHz})}$ (dB/cm)
PMMA 2	1.18	1.008	5.98		n.a.	
PMMA 3	1.19	1.001	5.96		n.a.	
PMMA 5	1.20	1.000	6.00	0.80	1.033	5.03
PMMA 7.5	1.17	1.002	5.87	0.69	1.649	5.12
PMMA 10	1.18	1.000	5.90	0.71	1.477	5.03
average	1.18	1.002	5.94	0.73	1.39	5.06
uncertainty	$\leq 1\,\%$	$\leq 0.4\,\%$	$\leq 1.1\,\%$	$0.06 = 8\,\%$	$0.32 = 23\,\%$	$\approx 24.4\,\%$

The calculated values for absorption parameters are shown in table 2 and figure 5. The standard deviation of the parameters was in all cases larger than the fit error and was therefore taken as uncertainty of the

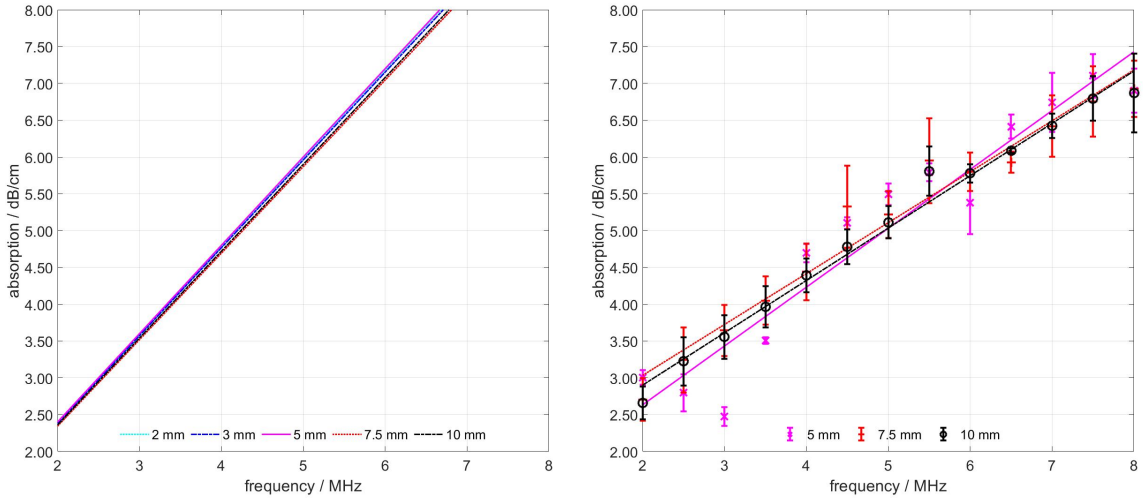

(a) Radiation Force Balance

(b) Hydrophone

Figure 5. Absorption of PMMA discs of different thicknesses as a function of frequency. The absorption was calculated with a numerical fit (equation 16) using the measured powers in case of the Radiation Force Balance and not with a fit of calculated absorption values at specific frequencies. Therefore no markers are shown in (a) but only the fit curves.

parameters.

5 DISCUSSION

The measured data corresponds to literature values from PMMA as shown in table 3.

Within the bandwidth of the transducer, the power showed the expected behavior (figure 4): The power decreases at the borders of the bandwidth frequencies and it also decreases with thicker PMMA discs due to more absorption. The half-wave layer effects could be seen in the radiation force balance method as predicted in equation 12. They are stronger the thinner the PMMA samples are due to less absorption. This is a direct result from equation 12. The frequency exponent of the absorption is, as expected, close to 1 since PMMA is a solid plastic without plasticizers.

Uncertainties are not mentioned in the publications. The main source of uncertainty in our experiments is at present the exchange of the sample between the reference and a sample measurement and subsequently slightly different placements and alignments of the accessories. For the hydrophone measurement even small alignment errors of the sample lead to diffraction of the sound field and refraction out of the hydrophone's sensitive area. In case of the radiation force balance this error is negligible since the distance from the sample to the target is small and since it covers the whole ultrasound field.

The calculated absorption of the PMMA discs is similar for the radiation force balance method and the hydrophone measurement. The differences are probably due to the above mentioned errors. As other research shows, the uncertainties are lower with the radiation force balance method. This is a result of

Table 3. Comparison of obtained PMMA data with literature. Shown are the density ϱ, speed of sound c, impedance Z, the frequency dependent absorption coefficient α and the absorption at 5 MHz. * values are calculated from the published data.

	ϱ (kg/m^3)	c (m/s)	Z (Mrayl)	α (dB/(cm MHz))	$\alpha_{(5\,\mathrm{MHz})}$ (dB/cm)
Carlson, 2003 [2]	1192	2750	3.28	1.06*	60.84 Np/m =5.28 dB/cm*
Bloomfield, 2000 [3]	$1.18 \cdot 10^3$	$2.74 \cdot 10^3$	3.23	1.1	5.5*
Cheeke, 2012 [4]	$1.18 \cdot 10^3$	$2.61 \cdot 10^3$	3.08	2.48*	12.4
RFB method	1186	2744	3.254	1.18	5.94

the large absorbing target (vs. a small receiving area when using a hydrophone) and due to the usage of long pulses and therefore more received power (vs. short pulses for the hydrophone measurement). Half-wave-layer effects can only be seen with the radiation force balance measurement when using long pulses.
Our research was done as a proof of concept and will be refined in the future.

6 CONCLUSIONS

In this proof-of-concept study we have shown that the radiation force balance method is suitable to measure the attenuation coefficient of a sample very accurately. The measurement of the sample's thickness, density, speed of sound, and absorption can be realized in the same measurement setup. The reported absorption values were obtained at room temperature in the frequency range 2 MHz to 8 MHz and compared with hydrophone measurements. The radiation force balance method uses very long pulses to use a larger ultrasound power for measurement and to take all transmitted echoes into account for attenuation calculations. The method seems suitable for all materials that partially transmit ultrasound and will be extended to other materials in the future.

ACKNOWLEDGMENTS

We want to thank the *Investitionsbank Sachsen-Anhalt* and the *European Regional Development Fund (ERDF)* to give financial support to the research and development project *CaPS* (Project-No. 1704/00064).

REFERENCES

[1] International Electrotechnical Commission. IEC CD 63081: Ultrasonics - Methods for the Characterisation of the 52 Ultrasonic Properties of Materials, 2018, 20-21.

[2] Carlson, J. E.; van Deventer, J.; Scolan, A.; Carlander, C. Frequency and temperature dependence of acoustic properties of polymers used in pulse-echo systems, Proc. IEEE Ultrason. Symp, 2003, 885-888.

[3] Bloomfield, P. E.; Lo W.-J.; Lewin, P. A. Experimental study of the acoustical properties of polymers utilized to construct PVDF ultrasonic transducers and the acousto-electric properties of PVDF and P(VDF/TrFE) films. IEEE trans. UFFC, 2000, 1397-1405

[4] Cheeke, J.D.N. Fundamentals and applications of ultrasonic waves. CRC Press, Ed. 2. 2012, 457.

[5] Tanaka, M.; Girard G.; Davis, R.; Peuto, A.; Bignell, N. Recommended table for the density of water between 0°C and 40°C based on recent experimental reports. Metrologia, 38, 2001, 301-309.

[6] Hsu, D. K.; Hughes, M. S. Simultaneous ultrasonic velocity and sample thickness measurement and application in composites. JASA, 92 (2), 1992, 669-675

[7] Bilaniuk, N.; Wong, G. S. K. Speed of sound in pure water as a function of temperature. JASA, 93 (3), 1993, 1609-1612.

[8] Brekhovskikh, L. M. Waves in layered media. Academic Press Inc., Vol. 16, Ed. 2, 1980, 18ff.

[9] International Electrotechnical Commission. IEC 61161:2013; Ultrasonics - Power measurement - Radiation force balances and performance requirements, 2013.

[10] Physikalisch Technische Bundesanstalt. Report on key comparison CCAUV.U-K3 for ultrasonic power - Final Report. Metrologia, 51 Tech. Suppl. 09001, 2014.